

Supplementary Information for
**Metasurface-enhanced Infrared Spectroscopy in multiwell
format for real-time assaying of live cells**

Steven H. Huang^{a*}, Giovanni Sartorello^a, Po-Ting Shen^a, Chengqi Xu^{b,c}, Olivier Elemento^{b*}, and Gennady Shvets^{a*}

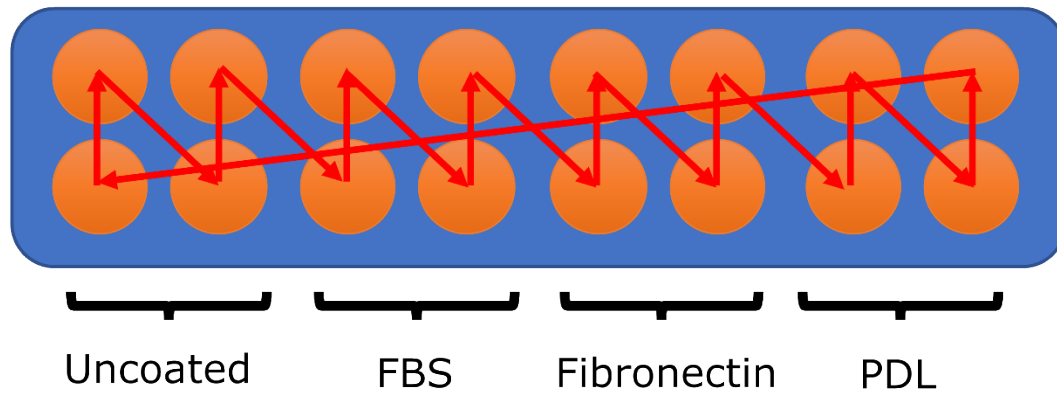
^a School of Applied and Engineering Physics, Cornell University, Ithaca, New York, USA 14853

^b Caryl and Israel Englander Institute for Precision Medicine, Weill Cornell Medicine, New York, NY, 10021

^c Meinig School of Biomedical Engineering, Cornell University, Ithaca, NY, 14853

*Email: hh623@cornell.edu, ole2001@med.cornell.edu, gshvets@cornell.edu

(a)



(b)

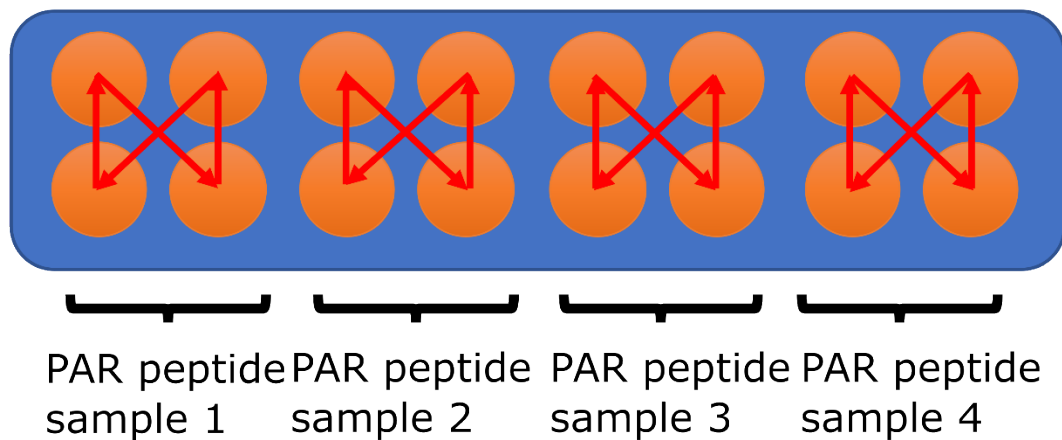


Figure S1. Stage movement pattern. (a) Cell adhesion measurement. 16 wells were probed in each cycle, with 16 minutes time resolution for each well. (b) PAR signaling measurement. 4 wells were probed in each cycle, with 4 minutes time resolution for each well. 4 cycles were used to cover the entire 16 well plate.

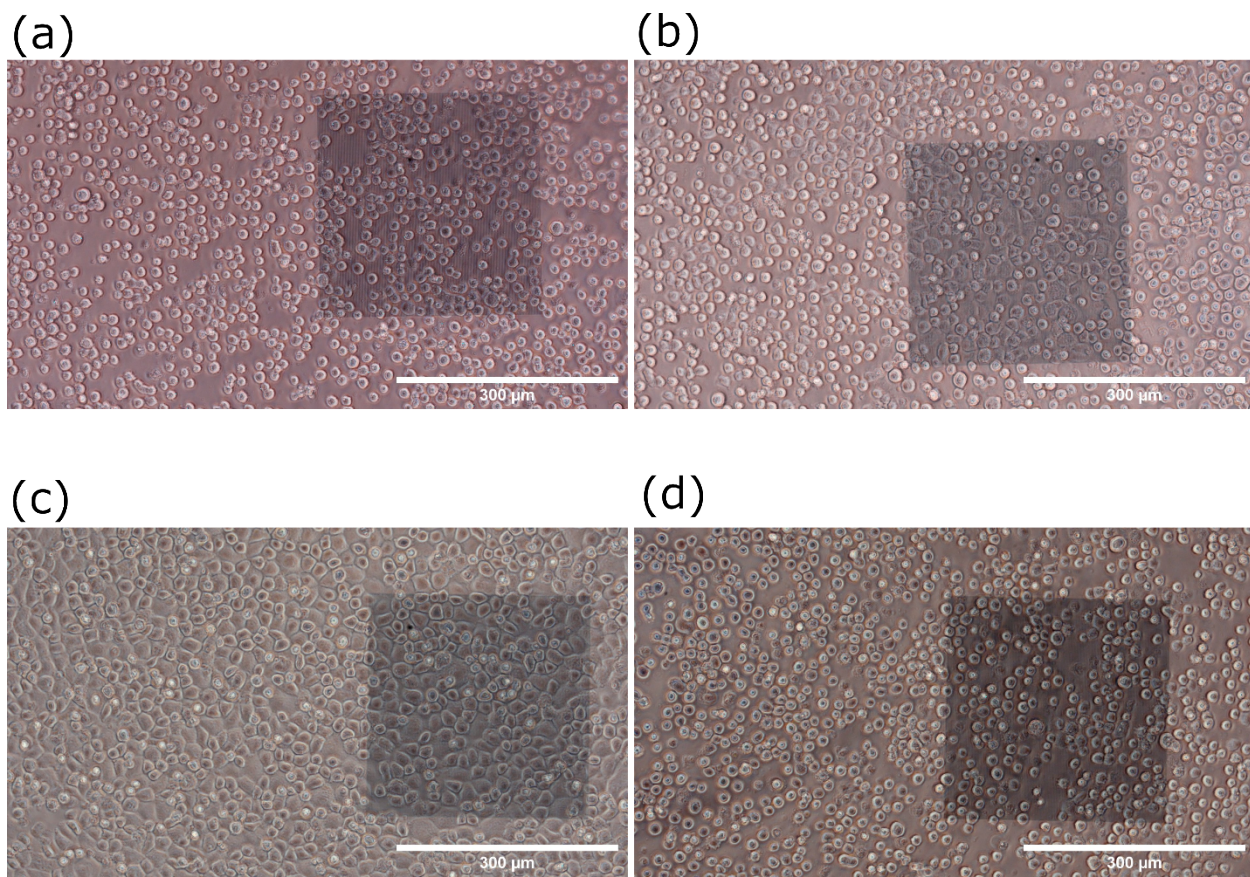


Figure S2. Phase contrast microscopy images of A431 cells on metasurface covered with different surface coatings. (a) no coating (b) 10% FBS (c) fibronectin and (d) poly-D-lysine. Scale bar: 300 μm . Clear difference in cell morphology can be seen, showing that whereas cells spread well for fibronectin and FBS coated metasurfaces, cell spreading is limited for uncoated and poly-D-lysine coated metasurfaces, consistency with the MEIRS result.

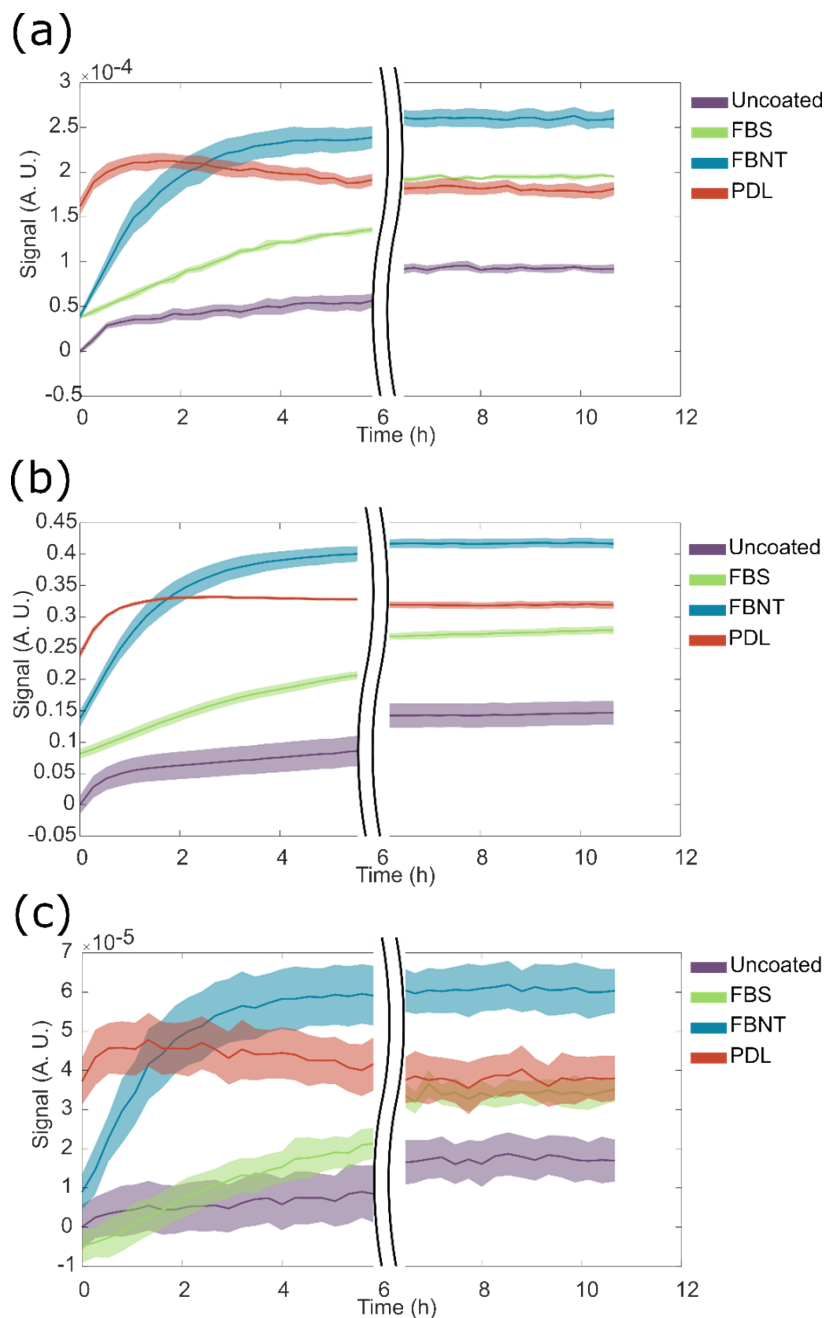


Figure S3. MEIRS measurement of A431 cell adhesion on metasurface with different surface coating for: (a) protein window, (b) plasmonic resonance window, and (c) lipid window. The same data as presented in Figure 4 of the main text, but instead of subtracting the spectrum at $t = 0$ from all subsequent spectra for each well (effectively setting the signal to zero at $t = 0$ for each curve), here the cellular signal curves are presented by subtracting the mean signal of uncoated wells at $t = 0$ from the signal of each well. The cellular signal here was obtained through linear regression by projecting the spectral data on the PC1 loading spectra presented in Figure 4 (a), (c), (e) of the main text. Presented this way, the contribution of the surface coatings to the IR absorption (and plasmonic resonance shift) signals are clear. PDL coating has a significantly larger contribution to the IR absorption signals compared with fibronectin and FBS coating.

PCA-LSTM model for spectral analysis and classification

Spectra have been entirely processed using the Scikit-learn (version 1.1.3) and Pytorch (version 1.13.0) for data analysis. We provide raw cell adhesion data and code available at https://github.com/Mew233/IRspectral/blob/master/spectral_PCA_LSTM-feats.ipynb. Cell adhesion data is a matrix with 656 rows (4 categories x 41 time points x 4 replicates) and 1200 columns (i.e., spectral variables).

The preprocessing steps included (i) Smoothing the FTIR spectra with Savitzky-Golay filter, (ii) applying PCA on selected window (proteins, plasmonic resonance, or lipids) to seek for the spectral variance among different coating samples and the main changes occurring in the time sequence, and (iii) arranging the spectral-temporal data for LSTM network development (Fig. S4). The first two PCs were selected to represent the original dataset. In protein window, the first two PCs explained 84.2% variance. They explained 99.0% variance in PR window, and they explained 97.2 % variance in lipid window. The input of the LSTM network is a two-dimensional vector with the size of 2 PCs x 41 timepoints for each replicate for each of the coating categories.

Arrange the multi-temporal-spectral data for inputting into the LSTM

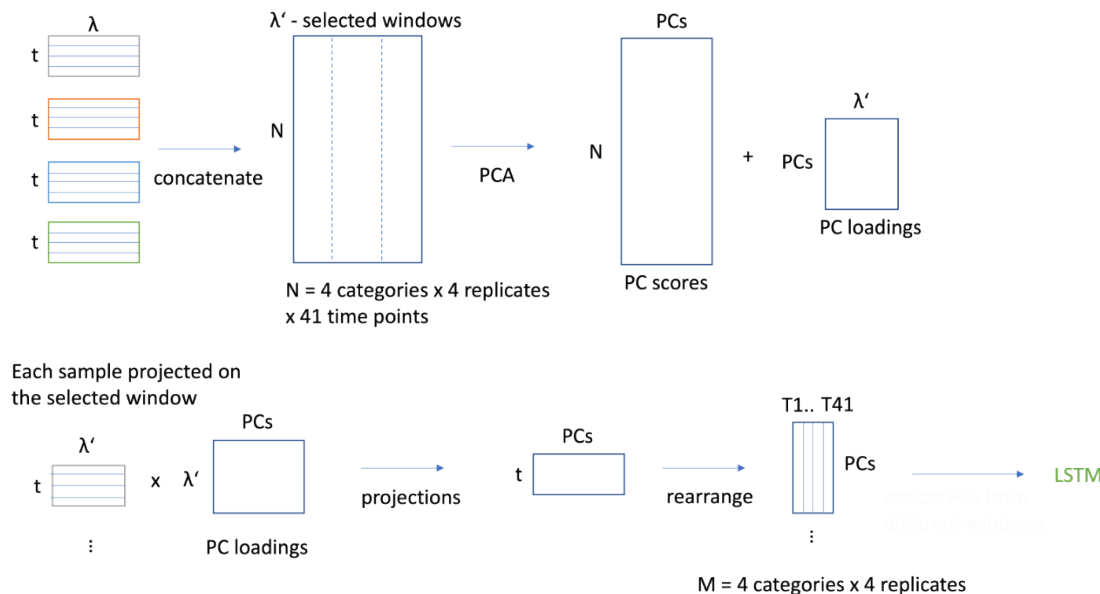


Figure S4. Data pre-processing for input into the LSTM model.

The structure of the long-short-term memory (LSTM) network (Figure S5) consists of an input layer, followed by a bidirectional long short-term memory (BiLSTM) layer, a dropout layer, a fully connected (FC) layer, a softmax layer, and finally an output layer. BiLSTM layer comes from the idea of recurrent neural networks (RNNs). RNNs have gained lots of attention for solving many challenging tasks especially for sequential or time series data analysis. RNNs have been applied in NLP code generation and music generation.^{1,2} However, RNNs can suffer from vanishing gradients problems when the information from earlier timepoints decay. LSTM network is therefore proposed to overcome this issue which selectively memorizes relevant information and forgets that is not relevant. A dropout layer is a regularization method to prevent model from overfitting. Features are merged by FC layer and the softmax layer computes the probability of the input data belonging to each certain class.

K-fold cross validation (K=4) method was applied to a subset of 12 samples (the remaining 4 samples were used to determine the ability of the model to predict new samples). The methodology generated 4

partial models (each from k-1 folds). Confusion matrix for the cross-validation dataset was obtained by summing the partial confusion matrices of each fold. Model hyperparameters are tuned by grid search and documented in Table S1.

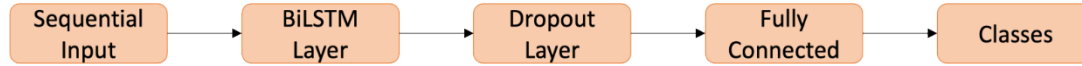


Figure S5. The architecture of LSTM model.

Hyper-parameters	Range	Optimal values
Learning rate	1e-4, 3e-4, 1e-3	3e-4
Dropout ratio	0.5, 0.2	0.5
LSTM layer number	1, 2	1
LSTM bidirectional	True	True
LSTM hidden dim	32, 64	64

Table S6. The hyperparameters used in our study.

References

1. Sun, Z. *et al.* A Grammar-Based Structural CNN Decoder for Code Generation. in *Proceedings of the Thirty-Third AAAI Conference on Artificial Intelligence and Thirty-First Innovative Applications of Artificial Intelligence Conference and Ninth AAAI Symposium on Educational Advances in Artificial Intelligence* (AAAI Press, 2019). doi:10.1609/aaai.v33i01.33017055.
2. Hadjeres, G. & Nielsen, F. Anticipation-RNN: Enforcing Unary Constraints in Sequence Generation, with Application to Interactive Music Generation. *Neural Comput. Appl.* **32**, 995–1005 (2020).